

## Dynamics of the reconstruction process Ir(100) $1 \times 1 \rightarrow 1 \times 5$

K. Heinz, G. Schmidt, L. Hammer, and K. Müller

*Institut für Angewandte Physik, Lehrstuhl für Festkörperphysik der Universität Erlangen—Nürnberg,  
Erwin-Rommel-Strasse 1, D-8520 Erlangen, Federal Republic of Germany*

(Received 11 February 1985)

The structure transition Ir(100)  $1 \times 1 \rightarrow 1 \times 5$  is observed by means of low-energy electron diffraction. After the preparation of the metastable and bulklike  $1 \times 1$  surface structure the transition is started by thermal activation at  $T > 800$  K. Diffraction spot profiles as well as integrated intensities are measured as a function of time for different constant temperatures. It is shown that streaks appear between integral-order spots from which superstructure spots develop. Both spot widths and intensities change rapidly in the beginning of the transition but subsequently vary very slowly without approaching their equilibrium value. A real-space model is proposed according to which linear atomic rows of the first layer are shifted from their initial quadratic hollow positions into hexagonal-close-packed arrangement. The activation energy of the transition is determined from the intensity increase to be  $W = 0.88 \pm 0.03$  eV.

### I. INTRODUCTION

The formation of a surface by cutting through the bulk solid leaves the surface atoms generally in nonequilibrium positions. A relaxation process towards the new minimum of free energy follows and ends in new equilibrium positions of the surface atoms whereby only the first few surface layers are involved. For metals in most cases only interlayer spacings normal to the surface are modified resulting in a damped oscillatory multilayer relaxation (for a recent survey see Ref. 1). At least for one example [Fe(211)] also an additional lateral shift of the first layer was observed.<sup>2</sup> However, the most drastic and striking relaxation process is that of reconstruction, where the symmetry of surface layers changes leading to more or less complicated superstructures. This behavior is mainly observed for semiconductor surfaces but also for a few metals, as e.g., Pt, Ir, Au, and W.

Structure determinations of such reconstructed surfaces by means of low-energy electron diffraction (LEED) are considerably complicated by the usually large surface unit cells which contain several atoms and lead to an increased number of diffraction beams. Nevertheless, it recently was possible to solve the structure of the reconstructed (100) surface of iridium, i.e., Ir (100)  $1 \times 5$ .<sup>3,4</sup> It was shown that the quasi-hexagonal model for that surface, which was proposed much earlier on the basis of LEED patterns,<sup>5,6</sup> is realistic. According to this model the top layer is nearly hexagonally close packed and fits to the substrate in bridge registry by puckering with an amplitude of about 0.5 Å.

In spite of this precise knowledge of the equilibrium structure, little is known about the structure transition  $1 \times 1 \rightarrow 1 \times 5$  itself, i.e., about the transition of the bulklike surface layer to the reconstructed phase. It is the purpose of this paper to give some information on the dynamics of this structure transition by means of LEED. Similar investigations exist for the Pt(100),<sup>7-9</sup> which also reconstructs into a nearly hexagonal close-packed structure.

An observation of the Ir(100) transition by means of work-function change was reported earlier.<sup>10</sup>

The investigation has to start with the preparation of the clean and nonreconstructed surface, which will be called  $1 \times 1$  in the following. This is described in the third section after experimental details have been given in the next section. The transition  $1 \times 1 \rightarrow 1 \times 5$  as observed by the development of integrated intensities as well as spot profiles is presented in the fourth section. Finally the data evaluation and discussion of the results follow.

### II. EXPERIMENT

The experiments were performed in an UHV equipment with a basic pressure of about  $10^{-10}$  mbar. However, as gas adsorption and desorption processes are necessary in order to prepare the  $1 \times 1$  phase (see Sec. 3), the residual gas pressure during the measurement was not better than  $10^{-9}$  mbar. The iridium crystal was oriented to within  $1^\circ$  of the (100) plane, mechanically polished and etched for 1 h in aqua regia. *In situ* preparation was performed by an 8 h bombardment with argon ions ( $\approx 3 \mu\text{A}/\text{cm}^2$ , 500 eV) followed by heating to 1600 K for 10 min. Appearing carbon could be removed by heating at 1300 K for 5–10 min in  $\text{O}_2$  at  $5 \times 10^{-7}$  mbar. A final tempering at 1300 K for 1 min led to a well-ordered reconstructed phase with sharp superstructure spots and no impurities detectable with Auger electron spectroscopy. The sample was mounted on a holder provided with an electron source for indirect heating which was possible up to 1800 K. The connection of the holder to a liquid-air reservoir through a thick copper lace allowed for temperatures down to 100 K.

The LEED experiment was performed using a classical four-grid optics. Integrated intensities and spot profiles were measured by means of a computer-controlled video system. This is described in more detail elsewhere<sup>11-13</sup> and so the description of the essentials is sufficient here. The video camera views the LEED pattern from outside

the UHV equipment and passes its signal to a processing computer via an interface. The computer can be made to create a rectangular electronic window of any wanted size on the pattern displayed on the monitor. The video signal within the window is digitized by the interface with a sampling rate of 75 nsec leading to a two-dimensional array of intensity pixels. From this, any intensity profile can be passed to the computer. If the window is programmed to surround a single diffraction spot the computer integrates the signals to the total spot intensity under simultaneous background subtraction at the window's edges. Due to fast assembler programming the whole procedure takes only 20 msec, i.e., the time of one television half-frame (European norm). Afterwards an external parameter as, e.g., the energy can be varied. The window is centered to the new spot position and the measurement procedure restarts. So, e.g., a 300 intensity-energy-points spectrum develops within 6 sec. A single profile at a fixed energy, i.e., a cut through the diffraction pattern, needs the same time as the integration to the total spot intensity which is 20 msec. Therefore, the time resolution with which dynamical processes can be observed with this video-LEED system is 20 msec. In other words, surface systems can be measured which vary with time constants considerably larger than 20 msec. As it will turn out below, this is the case for the structure transition Ir(100)  $1 \times 1 \rightarrow 1 \times 5$ .

### III. PREPARATION OF THE METASTABLE Ir(100) $1 \times 1$ SURFACE

As described in the last section the preparation of a clean Ir(100) surface results in the reconstructed  $1 \times 5$  phase which corresponds to thermodynamic equilibrium for the clean surface. In order to observe the transition  $1 \times 1 \rightarrow 1 \times 5$  the undisturbed  $1 \times 1$  configuration must be reestablished. It turns out that this is possible and that it corresponds to a metastable state which can be held quasistable at low temperatures. This is described schematically by the dependence of the free energy on the surface configuration given in Fig. 1. For zero coverage, i.e., for the clean surface, the absolute minimum corresponds to the reconstructed phase, whose  $1 \times 5$  pattern is given as well. If one understands the surface as a cut through the bulk, chemical bonds are cut when the surface is created. The subsequent relaxation leads to reconstruction in the case of Ir(100). Therefore, the basic idea to remove the reconstruction is to restore to some extent the bonds cut off. This is done by oxygen adsorption whereby we slightly modified treatments given in the literature.<sup>10,14</sup>

On the reconstructed face adsorption of  $O_2$  at  $5 \times 10^{-7}$  mbar is made to take place at 475 K for about 2 min. As shown in Fig. 1, the resulting diffraction pattern shows decreased intensities of superstructure spots with addi-

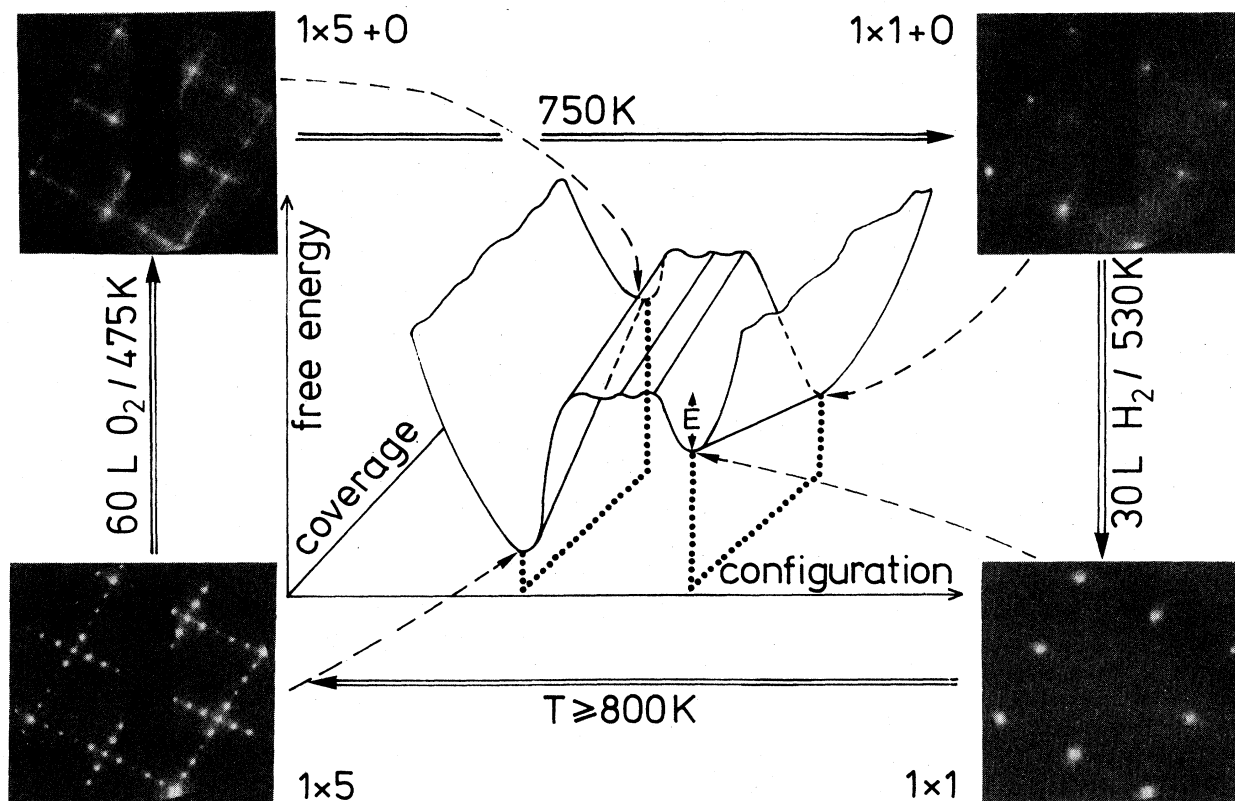


FIG. 1. Schematic behavior of the surface free energy as function of the surface configuration and coverage of oxygen. For the minima, the respective LEED patterns are displayed. The energy  $E$  is determined in Sec. V.

tional  $2 \times 1$  spots which are supposed to be caused by an oxygen superstructure. It also appears from the figure that the new state is assumed to be metastable. In fact, it turns out that heating to about 750 K makes the system overcome the activation energy with simultaneous removal of the reconstruction. The LEED pattern is now only  $1 \times 1$  corresponding to the absolute minimum of free energy. An increased background is observed which is believed to be due to disorderly adsorbed oxygen. Sometimes also faint  $2 \times 1$  oxygen superstructure spots are visible. In order to remove the oxygen, the sample is exposed to hydrogen at 530 K and  $5 \times 10^{-7}$  mbar for about 1 min. The reaction products desorb at this temperature and leave the clean, nonreconstructed surface which again corresponds to a metastable state. The structure appears to be practically stable for temperatures not exceeding 700 K. Some residual background and the widths of the diffraction spots indicate that the surface is not ideally ordered. Nevertheless, LEED intensity calculations on the  $1 \times 1$  surface could be very well matched to measured spectra as was shown in a separate paper.<sup>15</sup> A 2% first-to-second-layer contraction was found with a Zannazijona reliability factor<sup>16</sup> of  $r_{ZJ} = 0.079$ .

It should be emphasized at this point that the behavior of the free energy given in Fig. 1 is meant more schematic rather than quantitative. All that is important for the transitions observed is that the clean surface has a lower free energy in the  $1 \times 5$  phase compared to the  $1 \times 1$  phase and that the oxygen covered surface has a free energy which is higher in the  $1 \times 5$  phase compared to the  $1 \times 1$  phase. This can be verified as indicated in Fig. 1. However, it could also be due to, e.g., a decrease of the free energy upon adsorption for both phases. In this case the minimum for the  $1 \times 1$  phase must decrease more than that of the  $1 \times 5$  phase which is overtaken by the first one. Which of the various cases is true cannot be distinguished by our experiments.

After having prepared the clean  $1 \times 1$  phase as described, the transition  $1 \times 1 \rightarrow 1 \times 5$  can be started by flashing to temperatures above 800 K as also indicated in Fig. 1. The system overcomes the corresponding activation energy and reconstructs into the hexagonally close-packed  $1 \times 5$  structure.

#### IV. LEED INTENSITIES DURING THE TRANSITION $1 \times 1 \rightarrow 1 \times 5$

The transition from a metastable to a stable state suffers from the fact that the system is far from thermal equilibrium in the beginning and approaches the equilibrium state only for long times. So the transition process is temperature and time controlled. This means that no transition temperature can be defined, the transition cannot be described by giving a temperature dependence and it is irreversible. In this sense the transition of Ir(100) and similarly those of Pt and Au including the (110) faces differ from the transition W(100)  $1 \times 1 \leftrightarrow c(2 \times 2)$ . The latter was shown to develop with varying temperature only and to be reversible.<sup>17-19</sup>

To give a first overall impression of how the transition

can be followed by low-energy electron diffraction, the crystal was flashed to an elevated temperature for 10 sec and quickly cooled down to near 100 K afterwards in order to freeze the state reached. The resulting patterns are given in Fig. 2 starting with the  $1 \times 1$  phase [Fig. 2(a)] and followed by low-temperature photographs after a flash to 930 [Fig. 2(b)], 990 [Fig. 2(c)], 1050 [Fig. 2(d)], 1100 [Fig. 2(e)], and 1400 K [Fig. 2 (f)]. It turns out that an increased background develops and streaks along the edges of the unit cells appear. With the transition proceeding, the streaks become more and more structured and finally the superstructure spots are formed. However, the well-known  $1 \times 5$  pattern with sharp spots and low background develops only after a flash to about 1300 K or higher.

In order to avoid a mixing of time and temperature dependence of the transition process the crystal is flashed to an elevated temperature. In the case of beam profile measurements (Sec. IV A) this temperature is held constant for a certain period of time after which the state reached is frozen in by again cooling down to liquid-air temperature. Then, beam profiles are measured followed by another period of time and subsequent cooling. By this procedure, beam profiles result, which are only poorly affected by thermal diffuse scattering. On the other hand, integral intensities were taken (Sec. IV B) by heating the sample to an elevated temperature which then is held constant while the development of intensities with time is recorded.

#### A. Beam profiles

Figure 3 shows intensity profiles at 84 eV along the line between the 10 and 11 spots after a flash to 940 K. The times given in the figure correspond to the heating periods at 940 K, whereby the temperature increase itself took an extra of about 10 sec. Each heating cycle was started from the  $1 \times 1$  phase prepared as described above. The measurement itself was taken after quenching to liquid-air temperature subsequent to heating.

Confirming the visual impression from the photographs in Fig. 2, the background between the integer-order spots increases, i.e., streaks appear at the cost of the intensities of the  $1 \times 1$  structure spots. These streaks show a certain structure already in the very beginning of the transition. However, it clearly shows up that the streak maxima are not concentrated at the fifth-order positions. The streak structure changes during the transition leading only finally to the well-known superstructure spots.

The  $0\frac{6}{5}$  and  $\frac{6}{5}0$  spots (not shown in Fig. 2) appear at nearly the same positions throughout the transition and show Gaussian shape. Therefore the development of these spots was used for the beam profile analysis. It is shown in Fig. 4 for a constant temperature of 965 K and for different times after a flash to that temperature. As indicated by the inset in Fig. 4 the beam profiles were taken by surrounding spots wanted by a quadratic window. The existence of streaks between the integer-order spots is indicated by the hatched areas. For intensity reasons the video signal was horizontally integrated between the verti-

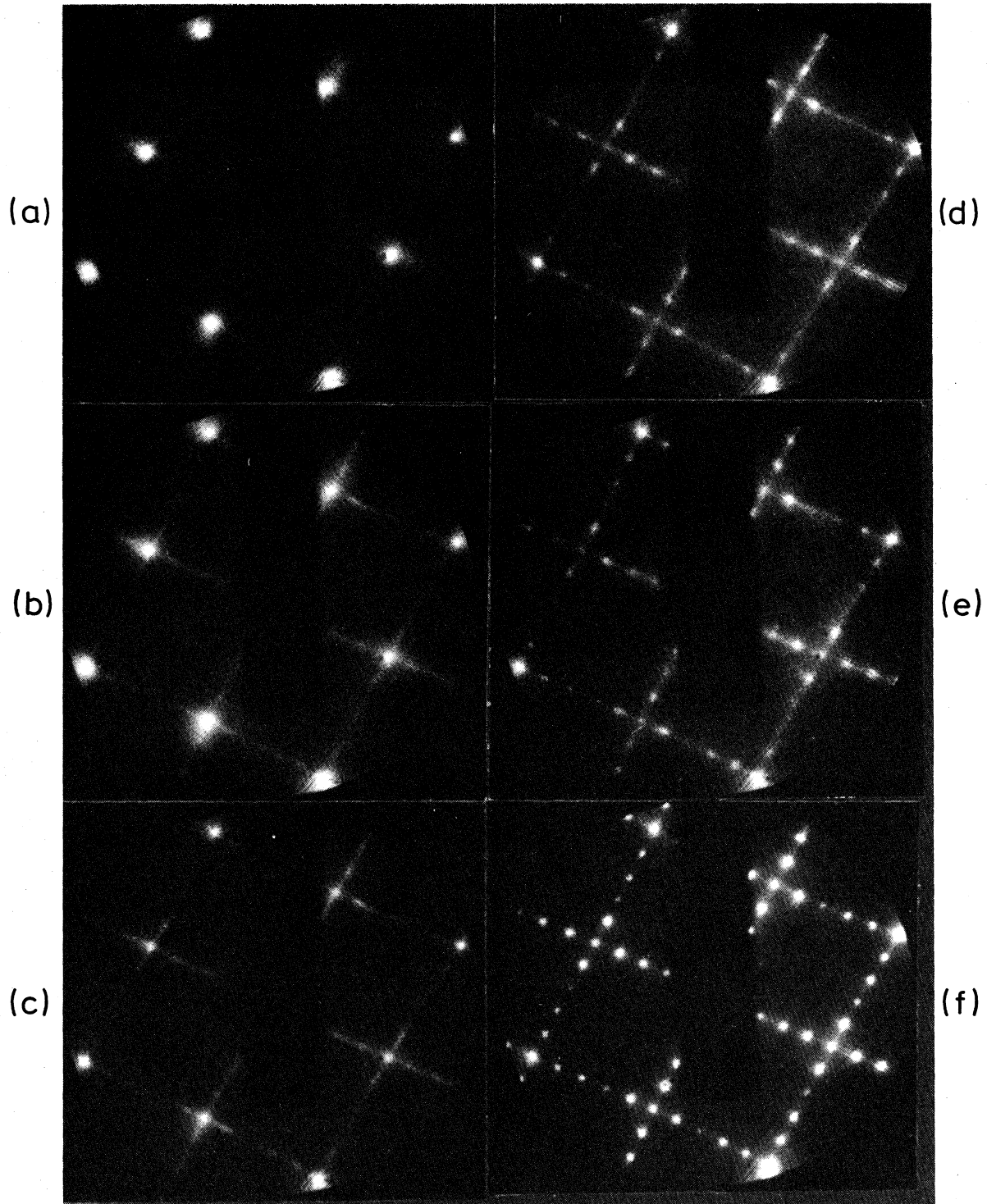


FIG. 2. (a) LEED pattern at 100 eV of the clean Ir(100)  $1 \times 1$  surface; (b)–(f) LEED patterns after a 10 sec flash to 930, 990, 1050, 1100, and 1400 K, respectively, taken after subsequent cooling to about 100 K.

cal window edges so that a vertical, but horizontally averaged profile results. Finally a constant background level is subtracted which is the average signal determined at the upper and lower window edges. Because of that subtrac-

tion procedure, the streak intensity is subtracted in case of the  $0 \frac{6}{5}$  spot but not for the  $\frac{6}{5} 0$  spot, which therefore appears to have higher intensities. Moreover, the resulting profiles are parallel and normal to the streak direction for

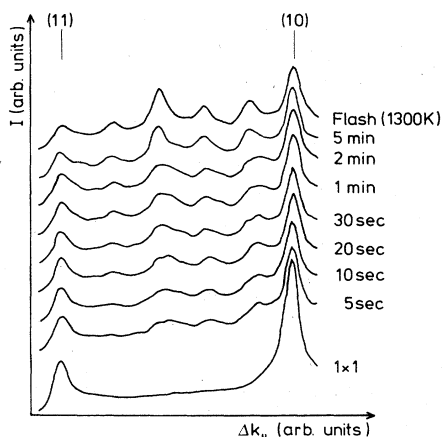


FIG. 3. Diffraction spot profiles at 84 eV along the line between the 10 and 11 spots for several times after a flash to 940 K. The measurement of each profile takes 20 msec.

the  $0\frac{6}{5}$  and  $\frac{6}{5}0$  spot, respectively. The measurements are taken at 99 eV and for normal incidence where both spots are symmetrically equivalent.

The evaluation of the data in Fig. 4 with respect to the beam half-widths is given in Fig. 5 in terms of percentages of the 10 reciprocal-lattice-vector length. The upper curve corresponds to the measured half-widths of the  $0\frac{6}{5}$  spot. It turns out that it decreases only very slowly except for the first part of the transition. Unfortunately, beam profiles could not be measured at the very beginning of the structure change because of the weakness of the sig-

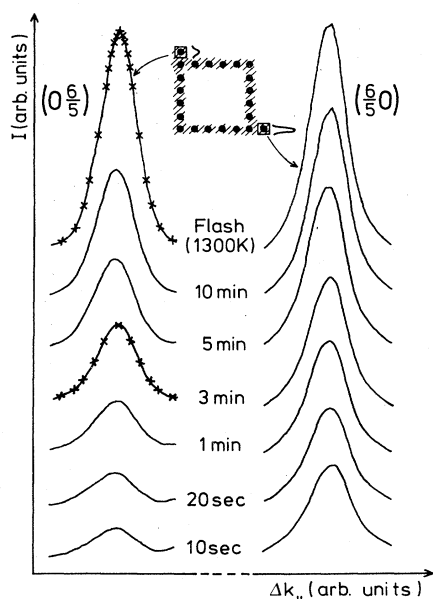


FIG. 4. Development of the  $0\frac{6}{5}$  and  $\frac{6}{5}0$  spot profiles at 99 eV and a temperature of 965 K. Crosses at two of the profiles were calculated assuming spots of Gauss shape. The inset gives the unit mesh of the diffraction pattern whereby streaks are indicated by hatched areas.

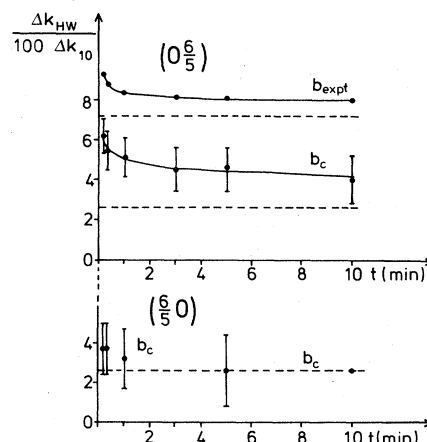


FIG. 5. Half-widths of the  $0\frac{6}{5}$  and  $\frac{6}{5}0$  spots as function of time in percentage units of the reciprocal unit mesh length  $k_{10}$ . The top curve corresponds to the experimental values as taken from Fig. 4. The curves below result by subtraction of the width of the instrument response function (see the text).

nal. In order to get an idea of the degree of long-range order during the transition, the measured beam width has to be corrected as it is broadened by the LEED instrument response function. It appears that the beam profiles show Gaussian shapes in good approximation (crosses for two profiles in Fig. 4) so the correction can be done by quadratic subtraction of the beam width produced by a (nearly) ideal surface. This was taken from the 10 and 11 beams of the unreconstructed surface and turned out to be  $(5.9 \pm 0.5)\%$  of the reciprocal unit mesh length. The result of the half-width correction is given below the experimental curve in Fig. 5 for both the  $0\frac{6}{5}$  and the  $\frac{6}{5}0$  spot. Error bars are given as well as resulting from the determination of the superstructure and integer-order spot widths. The dashed lines correspond to the widths which result after a flash to near or above 1300 K. For the  $0\frac{6}{5}$  spot, i.e., parallel to the streaks, this value is approached only after very long times. However, the width of the  $\frac{6}{5}0$  spot, i.e., normal to the streaks, seems to be practically constant at least within the error of measurement and takes its final value from the very beginning of the transition.

## B. Integrated intensities

The variation of integrated intensities has been measured for both superstructure and integer-order spots. The results are displayed in Fig. 6 for two temperatures in case of the 10 spot and for a whole set of temperatures for a superstructure spot; here, it is the  $0\frac{2}{5}$  spot. Different from the measurements of spot profiles the elevated temperature is maintained and the development of intensities with time is recorded at the constant temperature. All curves were taken at normal primary electron incidence and at an energy of 84 eV where both spots show considerable intensity in the reconstructed phase. The dashed vertical line indicates the time after which the temperature flash to the respective temperature is completed

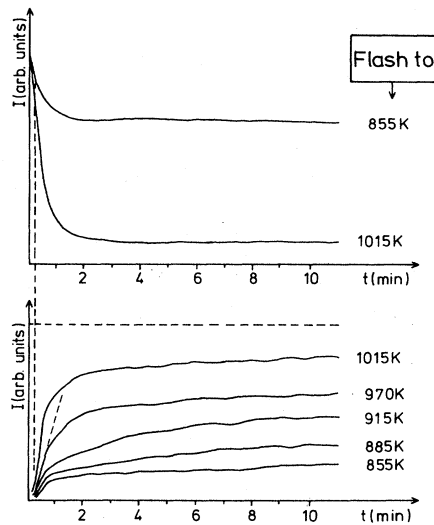


FIG. 6. Development of integer order and superstructure spot intensities with time for different temperatures. For the superstructure spot the influence of the Debye-Waller factor is eliminated. The horizontal dashed line gives the equilibrium intensity resulting after a flash to or above 1300 K. The vertical dashed line indicates the time after which the temperatures given are reached.

(about 10 sec). The superstructure spot intensities are corrected to cancel the influence of the Debye-Waller factor using a Debye temperature of 420 K.

It is evident from Fig. 6 that the superstructure spots develop at the cost of the integer-order spots as it is seen from the 10 intensity drop. The very first part of this drop, however, must at least partly be due to increased thermal diffuse scattering because of the temperature flash. Superstructure spots show a relatively steep and nearly linear increase at the beginning followed by a very slow further growth. Recently, a similar behavior was observed for superstructure spots of oxygen ordering on the W(112) surface.<sup>20</sup> It seems that for  $T \lesssim 1000$  K the equilibrium intensity value (dashed line) is not approached even within very long times but only after a flash to above 1300 K.

## V. DISCUSSION

The experimental results as described above can be summarized as follows.

The structural transition  $1 \times 1 \rightarrow 1 \times 5$  can be started from the metastable  $1 \times 1$  phase by thermal activation.

The transition starts by the formation of intensity streaks along the  $1 \times 1$  unit mesh edges.

Superstructure spots develop from these streaks at the cost of integer-order spots.

Half-widths of the growing spots are nearly constant normal to the streaks but decrease in the direction parallel to them.

Integrated intensities show a linear increase in the beginning followed by a very low further growing rate.

Even after long times integral intensities as well as

widths of superstructure spots do not approximate their equilibrium values. This happens only after a flash to near or above 1300 K.

The development of intensity streaks along the  $1 \times 1$  unit mesh edges indicates that at least partial disorder appears in the beginning of the transition. The streaks are interpreted to correspond to linear atomic rows which have no phase correlation. The position and direction of the streaks show that the rows are the same which, in case of strong correlation, build up the ordered  $1 \times 1$  phase. Therefore, as illustrated in Fig. 7, the transition is assumed to start from the ordered phase (upper part) via shifting of atomic rows (middle part) and to end finally by close packing of the rows (lower part) forming a nearly hexagonal unit mesh as seen from the top view. This reordering procedure from the disordered rows is consistent with the observation that the new superstructure spots develop from the streaks and that the spot half-widths normal to streaks is nearly constant corresponding to the average length of the rows. Of course the formation of streaks and superstructure spots happens at the expense of the integer-order spot intensities.

Of course the final quasihexagonally close-packed structure shows a higher density of surface atoms than the initial  $1 \times 1$  phase. Therefore, the formation of steps must be the consequence. However, the LEED pattern did not show any beam splitting or broadening as it is known to be caused by the existence of steps. Therefore it can be concluded that the average distance of steps must be of the order or larger than the coherence length of the primary beam, which is about 100 Å. If we take 100 Å as a rough estimate of a terrace width in the reconstructed phase the edge atoms have to diffuse about 15 Å according to the 15% more dense packing of the hexagonal arrangement compared to the quadratic one. One has to remember that this is only 5–6 at. diam. of iridium.

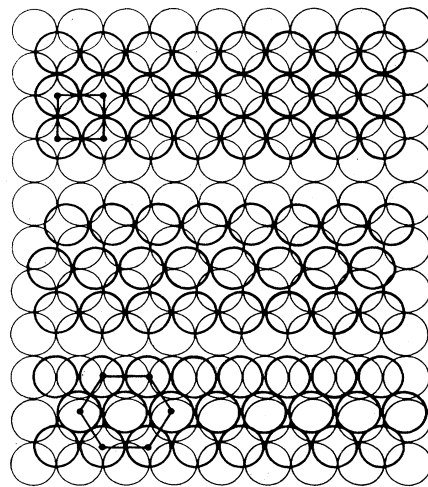


FIG. 7. Real space model of the transition starting at the  $1 \times 1$  phase (upper frame), with an intermediate state of disordered rows (middle), and ending in a hexagonal close-packed structure (bottom). First and second layer atoms are given by heavy and thin lines, respectively.

The ordering of the reconstructed phase must not be understood in terms of disordered rows clicking suddenly into a puckered hexagonal atomic arrangement. The forming of this quasihexagonal unit mesh is believed to develop via more or less heavily distorted hexagonal unit meshes. This picture is consistent with the fact that the position of superstructure spots is not well defined during the early part of the transition as it was demonstrated in Fig. 3. However, this could also be qualitatively explained by the existence of small reconstructed domains being mutually out of phase.

The decrease of the half-widths parallel to the streak direction corresponds to the growth of reconstructed domains in direction normal to the rows. Figure 5 shows that a considerable decrease happens only in the first part of the transition and is only followed by a very weak drop during the following part. This behavior is similar to the dependence of the integrated intensity as given in Fig. 6, where most of the intensity increase takes place within the first minute after the transitions start. Possibly the further evolution of the transition is impeded by the interaction of different domains touching each other. As integrated intensities at temperatures below 1000 K do not approach the final equilibrium intensity even at long times, a certain part of the surface or domains of it must be interpreted to resist switching into the final state of reconstruction. This might also be due to the existence of domain walls. Similar time dependences as described were also observed for the dynamics of other phase transitions as, e.g., in the case of oxygen on W(112).<sup>20</sup>

At the moment it is very difficult to extract more quantitative insight from the measured time dependences and this is so for several reasons. First of all in our case one cannot apply results based on lattice-gas calculations, although, e.g., Pott's model calculations predict slow evolutions of domain sizes as observed here. The reconstructed phase consists of a quasihexagonal, i.e., close-packed and puckered atomic arrangement on a quadratic substrate. This incommensurability implies that the surface atom positions do not coincide with lattice-gas positions of the quadratic substrate. Moreover, we cannot exclude that the domain growth is affected by surface defects as e.g., steps and vacancies. Formation of steps during the transition must even be assumed because the reconstructed phase is more densely packed than the surface layer of the  $1 \times 1$  phase. Long-distance mass transport, however, can only be avoided by step formation. Lastly, it must be emphasized that the initial  $1 \times 1$  state of the transition is a metastable state which is far away from thermal equilibrium at any temperature. In particular, no critical temperature can be defined.

The interpretation of intensity data is further complicated by the possibility that the Debye temperature of the first layer may change during the transition. Therefore, the Debye-Waller factor can vary although the temperature is held constant. Moreover, dynamic intralayer scattering of the growing reconstruction layer could cause intensities to be not strictly proportional to the number of

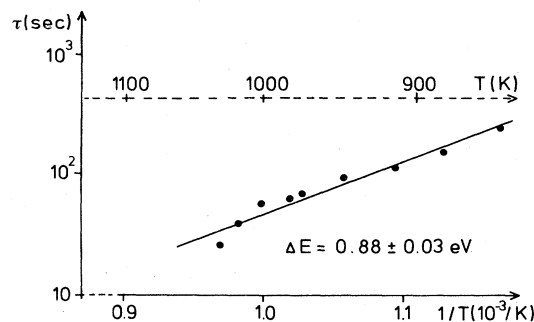


FIG. 8. Arrhenius plot of the characteristic times  $\tau$  of initial linear increase of the superstructure spot intensities of Fig. 6. The straight line gives an activation energy of 0.88 eV.

atoms in reconstruction positions.

If one assumes these latter possible effects to be negligible one can also extract quantitative information from the measured data. The superstructure spot intensity then depends linearly on the number of rows or atoms in the final atomic geometry. These rows must have shifted out of the atomic hollow positions of the  $1 \times 1$  phase, a process which costs activation energy  $E$  as indicated in the free-energy diagram of Fig. 1. Therefore, the time constant of this process is  $\tau \sim \exp(E/k_B T)$ . It appears that the total intensity increase with time cannot be described in terms of one single time constant or energy as already mentioned above. However, we can assume that, at least, at the very beginning the kinetics of the process is dominated by its activation energy. Therefore, the time constant of the very initial intensity increase in Fig. 6 should be identical to  $\tau$ . This is true for any order of the kinetics as long as the data evaluation is restricted to  $t \ll \tau$ . Therefore we interpret the initial slope of the  $I(t)$  curves in Fig. 6 as the time constant  $\tau$  as indicated, for example, for the 970 K curve by the dashed line. The corresponding Arrhenius plot in Fig. 8 indeed gives a straight line. From the slope of the line the activation energy  $E = (0.88 \pm 0.03)$  eV can be taken, whereby the error results from linear regression. This value is in fair agreement with that obtained by work-function measurements,<sup>10</sup> i.e.,  $E = 20 \pm 1$  kcal/mol  $\approx 0.87 \pm 0.04$  eV.

In conclusion, we could show that the structure transition Ir(100)  $1 \times 1 \rightarrow 1 \times 5$  develops by thermal activation via shifting of linear atomic rows. In an intermediate stage the rows are disordered giving streaks in the diffraction pattern. Superstructure spots develop from the streaks, i.e., in real space rows pack together to form quasihexagonal atomic arrangements. After a first rapid increase of reconstructed domain widths, the further evolution of reconstruction develops on a very long time scale. The same is observed through the development of integrated superstructure spot intensities. From their initial linear increase the activation energy for the transition  $E = 0.88 \pm 0.3$  eV is extracted.

- <sup>1</sup>J. Sokolov, F. Jona, and P. M. Marcus, *Solid State Commun.* **49**, 307 (1984).
- <sup>2</sup>J. Sokolov, H. D. Shik, U. Bardi, J. Jona, and P. M. Marcus, *Solid State Commun.* **48**, 739 (1983); *J. Phys. C* **17**, 371 (1984).
- <sup>3</sup>E. Lang, K. Müller, K. Heinz, M. A. Van Hove, R. J. Koestner, and G. A. Somorjai, *Surf. Sci.* **127**, 347 (1983).
- <sup>4</sup>W. Moritz, F. Müller, D. Wolf, and H. Jagodzinski, in *Proceedings of the 9th International Vacuum Congress (IVC-9) and the 5th International Conference on Solid Surfaces (ICCS-5)*, Madrid, (1983), p. 70.
- <sup>5</sup>A. Ignatiev, A. V. Jones, and T. N. Rhodin, *Surf. Sci.* **30**, 579 (1972).
- <sup>6</sup>P. Heilmann, K. Heinz, and K. Müller, *Surf. Sci.* **83**, 487 (1979).
- <sup>7</sup>P. R. Norton, J. A. Davies, D. K. Creber, C. W. Sitter, and T. E. Jackman, *Surf. Sci.* **108**, 205 (1981).
- <sup>8</sup>K. Heinz, E. Lang, K. Strauss, and K. Müller, *Appl. Surf. Sci.* **11/12**, 611 (1982).
- <sup>9</sup>K. Heinz, E. Lang, K. Strauss, and K. Müller, *Surf. Sci.* **120**, L401 (1982).
- <sup>10</sup>J. Küppers and H. Michel, *Appl. Surf. Sci.* **3**, 179 (1979).
- <sup>11</sup>P. Heilmann, E. Lang, K. Heinz, and K. Müller, in *Proceedings of the Conference on Determination of Surface Structure by LEED*, Yorktown Heights, New York, 1980 (Plenum, New York, in press).
- <sup>12</sup>K. Heinz and K. Müller, in *Structural Studies of Surfaces*, Vol. 91 of *Springer Tracts in Modern Physics*, edited by G. Höhler (Springer, Berlin, 1982).
- <sup>13</sup>K. Heinz, N. Bickel, G. Besold, and K. Müller, *J. Phys. C* **18**, 933 (1984).
- <sup>14</sup>T. N. Rhodin and G. Broden, *Surf. Sci.* **60**, 466 (1976).
- <sup>15</sup>G. Besold, K. Heinz, E. Lang, and K. Müller, *J. Vac. Sci. Technol. A1*, 1473 (1983).
- <sup>16</sup>E. Zanazzi and F. Jona, *Surf. Sci.* **62**, 61 (1977).
- <sup>17</sup>M. K. Debe and D. A. King, *Surf. Sci.* **81**, 193 (1979).
- <sup>18</sup>I. Stensgaard, L. C. Feldman, and P. J. Silverman, *Phys. Rev. Lett.* **42**, 247 (1979).
- <sup>19</sup>P. Heilmann, K. Heinz, and K. Müller, *Surf. Sci.* **89**, 84 (1979).
- <sup>20</sup>G.-C. Wang and T. M. Lu, *Phys. Rev. Lett.* **50**, 2014 (1983); *J. Vac. Sci. Technol. A2*, 1048 (1984).



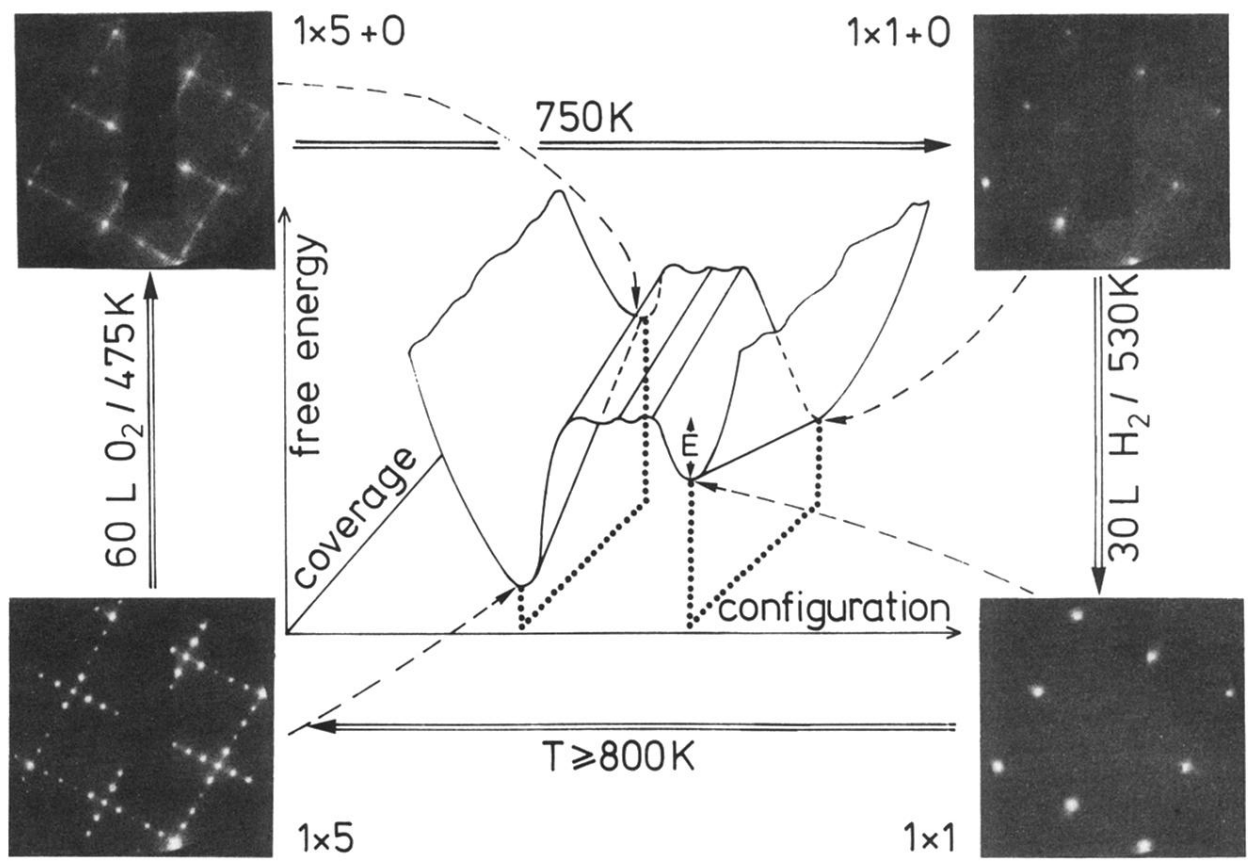


FIG. 1. Schematic behavior of the surface free energy as function of the surface configuration and coverage of oxygen. For the minima, the respective LEED patterns are displayed. The energy  $E$  is determined in Sec. V.

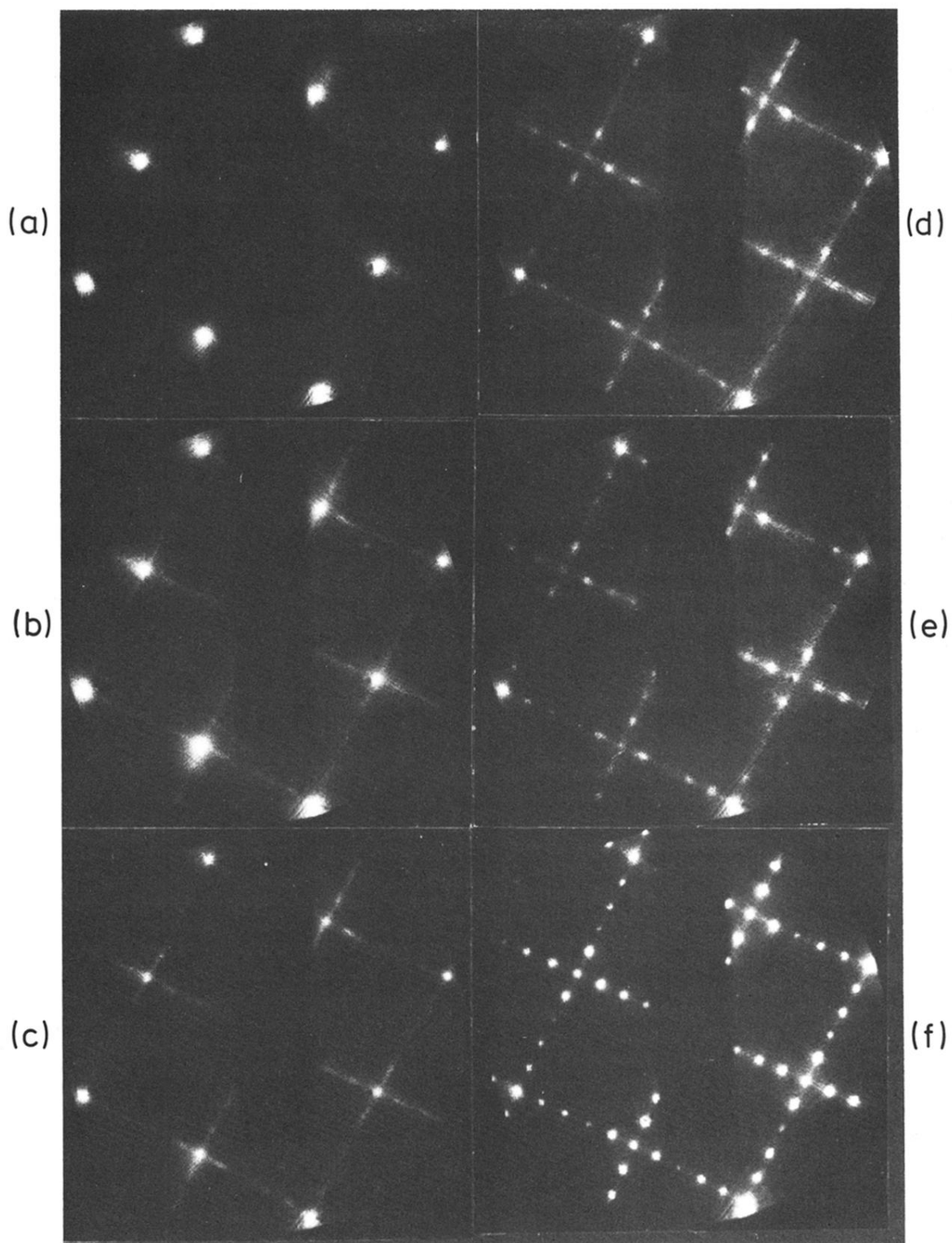


FIG. 2. (a) LEED pattern at 100 eV of the clean Ir(100)  $1 \times 1$  surface; (b)–(f) LEED patterns after a 10 sec flash to 930, 990, 1050, 1100, and 1400 K, respectively, taken after subsequent cooling to about 100 K.